

Visual Representation Learning from Unlabeled Video using Contrastive Masked Autoencoders

Jefferson Hernandez¹, Ruben Villegas², Vicente Ordonez¹

¹Rice University, ²Google Brain

{jefeher, vicenteor}@rice.edu, rubville@google.com

Abstract

Masked Autoencoders (MAEs) learn self-supervised representations by randomly masking input image patches and a reconstruction loss. Alternatively, contrastive learning self-supervised methods encourage two versions of the same input to have a similar representation, while pulling apart the representations for different inputs. We propose ViC-MAE, a general method that combines both MAE and contrastive learning by pooling the local feature representations learned under the MAE reconstruction objective and leveraging this global representation under a contrastive objective across video frames. We show that visual representations learned under ViC-MAE generalize well to both video classification and image classification tasks. Using a backbone ViT-B/16 network pre-trained on the Moments in Time (MiT) dataset, we obtain state-of-the-art transfer learning from video to images on Imagenet-1k by improving 1.58% in absolute top-1 accuracy from a recent previous work. Moreover, our method maintains a competitive transfer-learning performance of 81.50% top-1 accuracy on the Kinetics-400 video classification benchmark. In addition, we show that despite its simplicity, ViC-MAE yields improved results compared to combining MAE pre-training with previously proposed contrastive objectives such as VicReg and SiamSiam.

1. Introduction

Self-supervised visual representation learning has led to great success in image benchmarks [10, 28, 8, 27]. This success has been mainly driven by two paradigms: Joint-embedding methods and masked image modeling (MIM). Joint-embedding methods learn representations that are invariant to specific transformations, these methods are either contrastive [10, 28, 8], or negative free methods [12, 4]. More recently, masked image modeling has emerged as a successful alternative to joint embedding methods. These methods work by randomly masking out parts of the input and forcing a model to predict the masked parts [3, 27, 21, 55].

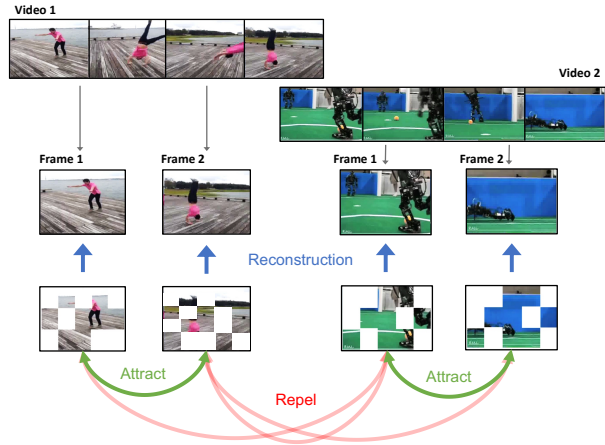


Figure 1: ViC-MAE operates over video frames using masked image modeling at the frame level and contrastive learning at the temporal level. Since our model operates over video frames, it can take advantage of viewpoint and temporal consistency which are absent in data augmentations over isolated images.

Self-supervised methods from the image domain have been successfully replicated for *video* representation learning with remarkable success [21, 55, 45, 22]. These methods yield strong video feature representations that transfer to a range of downstream video recognition tasks. However, there is still a gap in performance in the *video-to-image* transfer learning setting where it is difficult to obtain good image features by relying solely on video pre-training. Learning from video should also yield good image representations since videos naturally contain complex changes in pose, viewpoint, deformations, among others. These variations can not be simulated through the standard image augmentations used in joint-embedding methods or in MIM methods. In this work, we propose Video Contrastive Masked AutoEncoding (ViC-MAE) and show that our method improves *video-to-image* transfer performance while maintaining performance on video representation learning.

The work proposed by Gordeon et.al. [24] uses two distinct frames from a video as augmentations for instance discrimination similar to contrastive methods getting good results for video benchmarks but still relatively modest results in image benchmarks i.e. ImageNet. Feichtenhofer et.al. [21] uses a simple masked image modelling objective (pixel reconstruction) that obtains state-of-the-art results on video benchmarks and very strong results on ImageNet but still below the same method applied only on images. More recently, Parthasarathy et.al. [42] becomes the first to obtain results that rival ImageNet results by modifying the MoCLR [49] framework to videos using a larger crop size, temporal augmentations, and multi-scale contrastive pooling, but most importantly; this work devises a data collection methodology to address the domain mismatch. Given these encouraging results, we take a step back and ask the questions: Do we really need to collect more data to obtain good image representations from video? Are negative examples as used in [24, 42] actually needed to learn good video-to-image representations? Can we combine the simplicity of masked image modeling over the same frame and contrastive learning over different frames to learn global video representations?

With these question in mind, we propose to leverage contrastive learning and masked image modeling for videos in a single framework which we refer as ViC-MAE (Video Contrastive MAE). As illustrated in Figure 1, we sample two frames from a single video and use contrastive learning over the time dimension to make the representation learned by the encoder similar. This forces the encoder to learn a global representation for videos, and then we use masked image modeling over single frames with a simple reconstruction loss to encourage the encoder to also learn local features of the frames of the video. We also attempted to combine MAE with standard contrastive methods such as VicReg [4], and SiamSiam [12] by using the [CLS] token as a global video representation, but found that this simple strategy is insufficient to obtain good image recognition performance. Instead we propose to aggregate the local features learned by the MAE encoder using a global pooling layer. Then we use this aggregated global feature representation using a contrastive loss over this global video representation. We found this approach to be superior to using the [CLS] token. We use the ViT architecture [18] as our base model as this is the standard architecture used for previous masked image modeling methods [21, 55]. Our models are then finetuned for various image recognition tasks to demonstrate the transfer capabilities of our method. Based on our experiments, we report the following findings:

- (i) Training with large frame gaps improves image classification performance. Joint-embedding methods usually require strong augmentations, which in our video pre-training setting come naturally from choosing large gaps in between sampled frames.

- (ii) Training with negative pairs surpasses methods that only train with positive samples. This is in line with results for other methods that train on videos and evaluate on images [24, 42].
- (iii) Training with strong image transformations as augmentations is not necessary. This is in contrast to other works that still need to apply strong color and view augmentations to achieve good results [24, 42].

Our contributions can be summarized as follows: (1) We obtain the best *video-to-image* transfer learning results in the Imagenet-1k benchmark, (2) We propose ViC-MAE by combining contrastive learning with masked image modeling and show that our proposed method achieves superior accuracy than strong alternatives based on existing methods (VicReg, SiamSiam), and (3) We show superior transfer learning accuracy on a wide array of downstream image classification tasks compared to a baseline MAE pre-trained network.

2. Related Work

Our work is related to general self-supervised learning methods from video, and methods specifically targeting image representation learning from video in some form. In this section, we provide a summary for representative works.

Self-supervised learning from videos. Self-supervised learning in the video domain provides a way to exploit the time dimension as a learning signal that encourages models to learn a richer representation in comparison to learning only from images. In the past few years, this has involved the creation of pretext training tasks that leverage prior knowledge about videos such as frame continuity and forecasting [47, 52, 51, 37, 35, 17], object tracking [1, 53, 43, 54], and others. Other approaches also leverage facts about videos, but design the training in a contrastive learning paradigm [4, 12, 56, 58, 24, 42]. These methods leverage the temporal continuity of videos to sample negative and positive pairs for training under a contrastive learning objective. More recently, self-supervised learning approaches based on masked auto encoders (MAE) [27] rely on masked image modeling adapted to video data to pre-train models. These models can be later used for transfer learning to downstream tasks [21, 55, 50]. These methods train models by learning to reconstruct missing patches from a video in the form of either spatiotemporal patches or random patches. In contrast to the aforementioned works, our approach combines the discriminative representation learning of contrastive methods with the generative learning of masked image modeling methods in a unified pre-training strategy that is applicable to image and video downstream tasks.

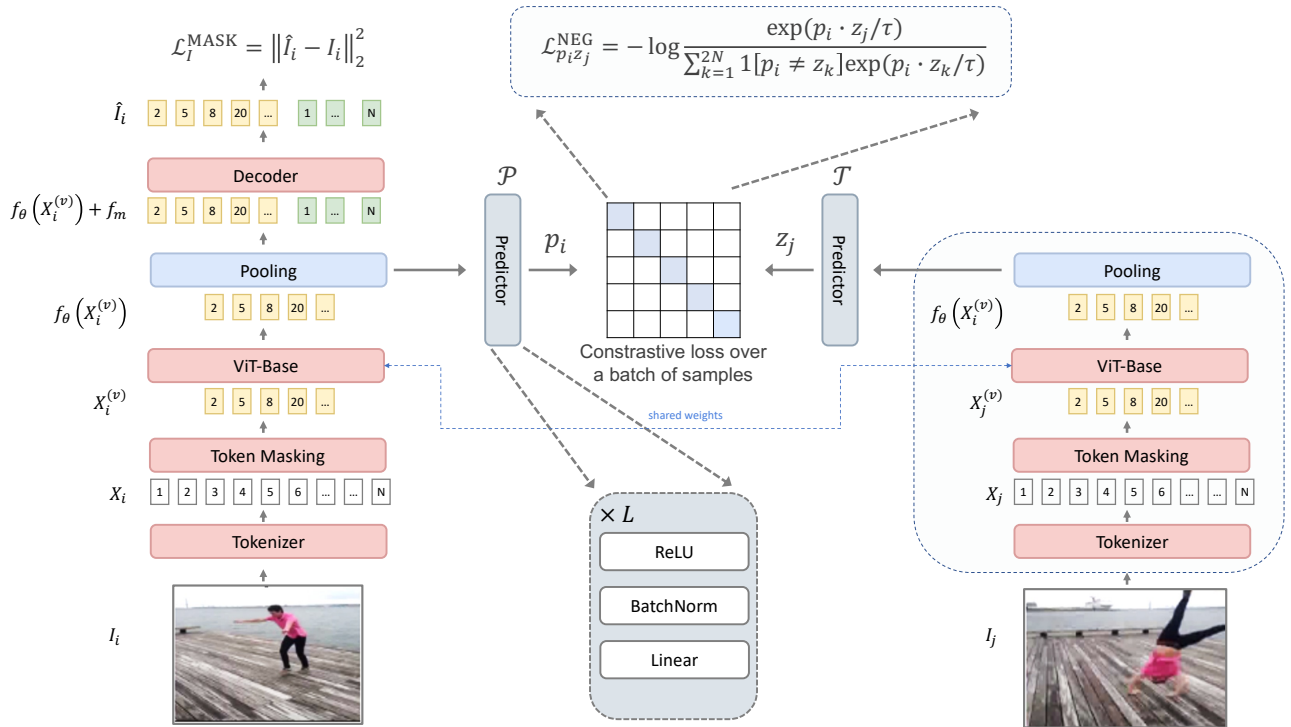


Figure 2: **ViC-MAE** inputs two distant frames from a video using a siamese backbone (shared weights), and randomly masks them, before passing them through a ViT-Base model which learns a representation of local features using masked image modeling. A global representation of the video is then constructed by global pooling of the local features learned by the ViT-Base model trained to reconstruct individual patches using an ℓ_2 loss. A standard predictor and a target encoder are used with a contrastive learning loss over the batch dimension to pull global representations closer for frames in the same video and push apart representations from frames in different videos. The use of an aggregation layer before the predictor network aids to avoid collapse of the learned global representations.

Learning image representations from video. While datasets such as ImageNet provide a large and diverse source of data for the development of perceptual systems, it still an incomplete representation of the world and how it is experienced by visual recognition models at test time. Image datasets lack a temporal dimension which provides a richer source of information for intelligent agents in the form of object deformations, temporal occlusions, multiple views, lighting changes, and more. This missing information causes models developed from image datasets to lack robustness when used in real world applications in which the inputs will be a continuous stream of frames in the form of video. To this end, there have been recent works that focus on learning robust image representations from video data. Video Contrastive Noise Estimation (VINCE) [24] argues that video provides natural image augmentations for free, and these can improve performance over artificially produced augmentations and even pretraining on ImageNet. Video Frame-level Similarity (VFS) [58] shows that using the time dimension to learn correspondences can produce models learned on video

datasets that transfer to downstream image tasks. In [56], they use cycle consistency that first maps an image from a video into a similar image to another video, and then map that image back to the closest frame within the initial video which could vary slightly from the origin of the cycle. Feichtenhofer et.al [21] uses masked visual modeling for video representation learning but the model is shown to be useful on image level tasks. More recently, Piergiovanni et.al. [44] proposed models that can simultaneously learn from image and video datasets while Parthasarathy et.al [42] proposes a video dataset curation procedure that addresses the domain mismatch between video and image datasets. In contrast, our method aims to learn representations from any video dataset using ViC-MAE which learns representations from video that generalize to both image and video datasets.

3. Method

We propose ViC-MAE for space-time feature learning, which works using contrastive learning at the time level and

masked image modelling at the space level.

3.1. Background

We provide here some background terminology and review of closely related methods that we build upon.

Masked image modeling. Masked image modeling provides a way to learn visual representations in a self-supervised manner. These methods learn representations by first masking out parts of the input and then training a model to fill in the blanks using a simple reconstruction loss. In order to do this, we use an encoder f_θ that takes the non-masked input and learns a representation x , such that a decoder d_ϕ can reconstruct the masked part of the input. More formally, let x be the representation learned by the encoder for masked image I with mask M such that $f_\theta(I \odot M)$. A decoder d is then applied to obtain the first loss over masked and unmasked tokens $d_\phi(x)$. This defines the following reconstruction loss which is only computed over masked tokens:

$$\mathcal{L}_I^{\text{MASK}} = \|d_\phi(f_\theta(I \odot M)) \odot (1 - M) - I \odot (1 - M)\|_2^2. \quad (1)$$

Contrastive learning. In common image-level contrastive methods, learning with negatives is achieved by pushing the representation of the positive pairs (different augmented views of the same image) to be close to each other while pulling the representation of negative pairs further apart. More formally, let I and I' be two augmented views of the same image. Contrastive learning uses a siamese network with a predictor encoder \mathcal{P} and a target encoder \mathcal{T} [58, 10]. The output of these networks are l_2 -normalized to be $p = \mathcal{P}(I)/\|\mathcal{P}(I)\|_2$ and $z = \mathcal{T}(I')/\|\mathcal{T}(I')\|_2$. Given a positive pair from a minibatch of size N , the other $2(N - 1)$ examples are treated as negative examples. The objective then is to minimize the Info-NCE loss as defined in [40]. When learning with negatives \mathcal{P} and \mathcal{T} typically share the same architecture and weights.

Negative-free representation learning. Global visual representation learning without negative examples has been achieved recently using a variety of methods, achieving similar performance to contrastive learning methods. By not using negative examples, the objective becomes simpler, just minimizing the cosine feature distance for two different views of the same input. The issue with this type of optimization is that it can lead to representation collapse [26, 12]. There are several ways to avoid representation collapse such as the methods proposed by Chen et al. [12] (SiamSiam) and Bardes et al. [4] (VicReg). SiamSiam introduces an asymmetry between the predictor encoder \mathcal{P} and the target encoder \mathcal{T} by adding one extra multi-layer perceptron to the predictor encoder to stop the gradients that are backpropagated

from the loss of the target network. VicReg instead uses two regularization terms: (i) A term that maintains the variance of each embedding dimension above a threshold, and (ii) A term that decorrelates each pair of variables. The variance term (i) forces the embedding vectors of samples within a batch to be different while the covariance term (ii) prevents the collapse of the representations.

3.2. Combining MAE with Contrastive Methods.

One trivial way to combine MAE with contrastive learning methods is to use the [CLS] token of the transformer as a global video feature representation. This representation allows us to use any contrastive learning loss without modifications to the underlying ViT-B/16 transformer encoder.

This combination works as follows: Sample two frames I_i, I_j from a video and perform patch-level masking. The two frames are processed by the ViT-B/16 model f_θ producing token representations $f_\theta(I_i) = \{x_i^{\text{CLS}}, x_i^1, x_i^2, \dots, x_i^L\}$, where L is the sequence length of the transformer model. This is divided into two disjoint sets. The set $\{x_i^1, x_i^2, \dots, x_i^L\}$ represents the local features of the frame i and are used for masked image modeling following Eq. 1. Then, the x_i^{CLS} token can be used as a global representation with a contrastive loss.

We experiment with this approach using the SiamSiam loss [12] and the VicReg loss [4]. We review here these methods and how to combine them with MAEs, but the reader is referred to the original works for a more in-depth explanation of these methods [12, 4].

SiamSiam. A combination of SiamSiam and MAE, which we refer to as *MAE + SiamSiam* uses the x_i^{CLS} token which represents the global video representation as follows: We pass x_i^{CLS} to a projector network \mathcal{P} to obtain $p_i \triangleq \mathcal{P}(x_i^{\text{CLS}})/\|\mathcal{P}(x_i^{\text{CLS}})\|_2$. A similar procedure is followed for frame j , but the global representation is not passed to the projector network \mathcal{P} in order to obtain $z_j \triangleq x_j^{\text{CLS}}/\|x_j^{\text{CLS}}\|_2$. The SiamSiam objective is then applied as follows:

$$\mathcal{L}_{p_i, z_j}^{\text{SiamSiam}} = \|p_i - z_j\|_2^2 = 2(1 - p_i \cdot z_j). \quad (2)$$

VicReg. A combination of VicReg and MAE, which we refer to as *MAE + VicReg* uses the x_i^{CLS} token which represents the global video representation as follows: We pass it to a projector network \mathcal{P} to obtain $p_i \triangleq \mathcal{P}(x_i^{\text{CLS}})/\|\mathcal{P}(x_i^{\text{CLS}})\|_2$, we repeat this procedure for frame j using the target network \mathcal{T} to obtain $z_j \triangleq \mathcal{T}(x_j^{\text{CLS}})/\|\mathcal{T}(x_j^{\text{CLS}})\|_2$. The loss is calculated at the embedding level on p_i and z_j . The video frames are processed in batches, let us denote $P = [p^1, \dots, p^n]$ and $Z = [z^1, \dots, z^n]$, where each p^m and z^m are the global representation of video m after the projector network and target network respectively in a batch of size n vectors of dimension d . Let us denote by p_l the vector composed of

each value at dimension l in all vectors in P . The variance loss of VicReg is then calculated as follows:

$$v(P) = \frac{1}{d} \sum_{l=1}^d \max(0, \gamma - S(p_i, \epsilon)), \quad (3)$$

where $S(z, \epsilon) = \sqrt{\text{Var}(z) + \epsilon}$ and γ is a constant target value for the standard deviation, fixed to 1. The covariance loss of VicReg can be calculated as:

$$c(P) = \frac{1}{d} \sum_{l \neq k}^d [\text{Cov}(p^m)]_{l,k}^2, \quad (4)$$

where $\text{Cov}(p^m) = \frac{1}{N-1} \sum_m (p^m - \bar{p})(p^m - \bar{p})^T$. The final VicReg loss over the batch is defined as:

$$\mathcal{L}_{p_i, z_j}^{\text{VicReg}} = \frac{\lambda}{n} \|p_i - z_j\|_2^2 + \mu [v(P) + v(Z)] + \nu [c(P) + c(Z)]. \quad (5)$$

We perform experiments using these two combinations of MAE and contrastive losses as baseline comparisons for our method but found them to be underperforming with only contrastive or only masked methods. In other words, it is not trivial to adapt contrastive learning methods to be used in combination with masked autoencoders.

3.3. VIC-MAE

Building on masked image modeling and image-level similarity learning, we propose to learn spatio-temporal representations by using masking image modeling at the frame level and image level similarity at the time level. This means that each video frame is pulled towards a global video representation in the latent space. This can lead to representations that are invariant to object deformations, appearance changes and viewpoint variations. See Figure 2 for a general overview of our model.

Given a video with T frames $\{I_1, I_2, \dots, I_T\}$, we sample two frames I_i, I_j as a positive pair input during one step of training. After an input image tokenizer layer we obtain a set of patch-level token representations X_i and X_j for each frame. Then, we apply token masking by generating a different random mask M_i and M_j and apply them to both of the corresponding input frames to obtain a subset of input visible tokens $X_i^{(v)}$ and $X_j^{(v)}$. These visible token sets are then forwarded to a ViT encoder which computes a set of representations $f_\theta(X_i^{(v)})$ and $f_\theta(X_j^{(v)})$ respectively. Finally, for the first frame we compute $\hat{I}_i = d_\phi(f_\theta(X_i^{(v)} + f_m))$ where we have added a mask token f_m to let the decoder know which patches were masked and allows to predict patch-shaped outputs through \hat{I}_i . These output patches are then trained to minimize the ℓ_2 loss with the true patches in the input image:

$$\mathcal{L}_i^{\text{MASK}} = \|\hat{I}_i - I_i\|_2^2. \quad (6)$$

So far we have described only a standard masked autoencoder (MAE). In order to apply contrastive pre-training we use a separate prediction branch in the network by applying a global pooling operator Ω over the output representations $f_\theta(X_i^{(v)})$ from the main branch and $f_\theta(X_j^{(v)})$ from the siamese copy of the network. This step simplifies the formulation of our method and avoids using additional complicated losses or the `gradient-stop` operator to avoid feature representation collapse since the pooled features can not default to the zero vector as they also are being trained to reconstruct patches. We experiment using various aggregation methods including *mean* pooling, *max* pooling, and *generalized mean* (GeM) pooling [46].

These global representations are then forwarded to a predictor encoder \mathcal{P} and a target encoder \mathcal{T} to obtain frame representations:

$$p_i \triangleq \mathcal{P}(\Omega(f_\theta(X_i^{(v)}))) / \|\mathcal{P}(\Omega(f_\theta(X_i^{(v)})))\|_2,$$

and

$$z_j \triangleq \mathcal{T}(\Omega(f_\theta(X_j^{(v)}))) / \|\mathcal{T}(\Omega(f_\theta(X_j^{(v)})))\|_2$$

respectively. The predictor network \mathcal{P} and target network \mathcal{T} are symmetrical and we use standard blocks designed for contrastive learning [4, 10, 12]. These blocks consist of a Linear \rightarrow BatchNorm1d \rightarrow ReLU block repeated 2 times. From these representations, we apply the InfoNCE contrastive learning loss as follows:

$$\mathcal{L}_{p_i, z_j}^{\text{NEG}} = -\log \frac{\exp(p_i \cdot z_j / \tau)}{\sum_{k=1}^{2N} \mathbb{1}[p_i \neq z_k] \exp(p_i \cdot z_k / \tau)}, \quad (7)$$

where the denominator includes a set of negative pairs with representations z_k computed for frames from other videos in the same batch, $\mathbb{1}[p_i \neq z_k] \in \{0, 1\}$ is an indicator function evaluating to 1 when $p_i \neq z_k$ and τ denotes a temperature parameter.

The final loss is $\mathcal{L} = \mathcal{L}^{\text{MASK}} + \lambda \mathcal{L}^{\text{NEG}}$, where λ is a hyperparameter controlling the relative influence of both losses. In practice, we use an schedule to gradually introduce the contrastive loss and let the model learn good local features at the beginning of training.

4. Experiment Settings

We perform experiments to demonstrate the performance of our method on fine-tuning tasks on the ImageNet benchmark, as well, as other image recognition datasets. For reference we also evaluate our method on the Kinetics dataset for action recognition to show that our model is able to maintain performance on video benchmarks. Full details are in Appendix A.

Architecture. We use the standard Vision Transformer (ViT) architectures [18] and conduct experiments fairly across

Method	Pre-train.	ImageNet-1K		Kinetics-400 †	
		Top-1	Top-5	Top-1	Top-5
Scratch	-	71.39	88.45	-	-
TubeViT [44]	K600	81.40	-	88.6	97.6
MAE [21, 27]*	K400	81.34	95.4	81.3	94.9
ViC-MAE (ours)	K400	82.80	96.6	81.5	95.1
ViC-MAE (ours)	MiT	82.98	96.8	81.0	94.6

Table 1: **Transfer learning results from video pre-training to the ImageNet dataset.** The pre-training data is a video dataset (MiT, K600 or K400). All self-supervised methods are evaluated end-to-end with supervised finetuning on IN1K. Best results are in bold. †Kinetics-400 results are from models trained on any of the aforementioned video datasets and evaluated on a Kinetics-400. (*) The transfer results from Kinetics-400 to ImageNet-1K for MAE were obtained by replicating the results based on correspondence with the original authors.

benchmarks and methods using the ViT-B/16 configuration. For masked image modeling we use a small decoder as proposed by He et.al [27]. For the contrastive learning part we experiment with two alternatives.

- *MAE + {SiamSiam or VicReg}*. The predictor consists of the backbone network f_θ and a projector followed by a predictor as in Bardes et.al [4]. The target encoder consists of the backbone f_θ and the projector, which are shared between the two encoders.
- *ViC-MAE*. The predictor and the target networks share the same architecture consisting of the backbone network f_θ and a projector following Bardes et.al [4].

When using the MAE + {SiamSiam or VicReg} combinations, we use the [CLS] token from the ViT architecture which is typically used to capture a global feature from the transformer network and is used to fine-tune the network for downstream tasks such as classification.

Pre-Training. We adopt the Moments in Time [38] and the Kinetics-400 dataset [30] for self-supervised pre-training. They consist on $\sim 1000K$ and $\sim 300K$ videos of varied length respectively. We sample frames from these videos using distant sampling, which consists of splitting the video in non-overlapping sections and sampling one frame from each section. Frames are resized to 224px size, horizontal flipping and random cropping with a scale range of $[0.5, 1]$, are used as the only data augmentation, unless specified otherwise.

Settings. ViC-MAE pre-training follows previously used configurations [27, 21]. We use the AdamW optimizer with a batch size of 512. We evaluate the pre-training quality by end-to-end finetuning. When evaluating on video datasets we follow the common practice of multi-view testing: taking K

Method	ImageNet-1K	
	Top-1	Top-5
MAE [27] + SiamSiam [12]	58.58	82.88
MAE [27] + VicReg [4]	63.86	84.07
ViC-MAE (ours)	67.66	86.22

Table 2: **Combining MAE and contrastive methods is not trivial.** Linear evaluation on the ImageNet-1K dataset using types of contrastive learning. We use the [CLS] token as the global video representation and apply common contrastive methods, but these do not result on the best performance, which is obtained with our method.

temporal clips ($K = 7$ on Kinetics) and for each clip taking 3 spatial views to cover the spatial axis (this is denoted as $K \times 3$). The final prediction is the average of all views.

5. Results and Ablations

We first perform experiments to analyze the different elements of the ViC-MAE framework. All the experiments are under the *learning with negative pairs* setting using mean pooling over the ViT-B/16 features unless specified otherwise. Linear evaluation and end-to-end finetuning runs are done over 100 epochs.

5.1. Main result

Our main result evaluates *video-to-image* transfer learning and we use as our testbed the ImageNet-1K benchmark. We present our results in Table 1, along with video downstream accuracy on Kinetics-400. We compare ourselves fairly to previous reported results in the literature that also use the ViT/B-16 backbone. The previous reported state of the art comes from the work of Piergiovanni et al. [44], which use a novel Tube sampling methodology that allows them to train on video and images at the same time and obtains 81.40% top-1 accuracy on end-to-end finetuning transferring from the Kinetics-600 dataset. Our method surpasses this result by an absolute improvement of 1.58% points of accuracy transferring from the Moments in Time dataset. However TubeViT is still the best model under a ViT/B-16 architecture on the Kinetics-400 benchmark. Another key result from this table is that our method even when trained on Kinetics-400 still performs best than other methods in *video-to-image* transfer. Other previous results on the same problem that use different backbones include the works of Gordon et al. [24], Xu & Wang [58], and Wu & Wang [56]. However these all use a ResNet-50 backbone and obtain 54.5%, 33.8%, and 55.6% top-1 accuracies on linear evaluation. Since those works are not using the same setting we chose not to include them alongside the others.

Model	Pre-train.	Food	CIFAR10	CIFAR100	Birdsnap	SUN397	Cars	Aircraft	VOC2007	DTD	Pets	Caltech101	Flowers
MAE [27] ‡	K400	74.54	94.86	79.49	46.51	64.33	60.10	63.24	83.07	78.01	89.49	93.28	93.38
MAE [27] ‡	MiT	76.23	94.47	79.50	47.98	65.32	59.48	60.67	83.46	78.21	88.42	93.08	94.17
ViC-MAE (ours)	K400	76.56	93.64	78.80	47.56	64.75	58.96	60.14	83.74	78.53	87.65	92.27	93.35
ViC-MAE (ours)	MiT	77.39	94.92	79.88	48.21	65.64	59.76	60.96	84.77	79.27	88.85	93.53	94.62

Table 3: **Comparison of transfer learning performance of our approach** with supervised baselines across 12 natural image classification datasets. All results correspond to linear evaluation. Best results are shown in bold. ‡MAE trained on MiT and K400 randomly sample a frame from the video to compute a reconstruction loss; these models are trained and evaluated by us.

Combining MAE with contrastive learning is non trivial, and we set to test these by comparing our model with MAE models with alternative contrastive learning objectives SiamSiam [12] and VicReg [4]. We present our results using linear evaluation on Table 2. We use the [CLS] token as the global video representation for contrastive pre-training. We can notice in this table that competing methods underperform compared to our model which uses pooling of the local features by an absolute margin of $> 3\%$ over the MAE + VicReg model. See Appendix B for an evaluation of our method against baselines that combine MAE with contrastive learning on the problem of semi-supervised learning on ImageNet.

5.2. Transfer learning performance.

We evaluate transfer learning performance of our model across a diverse array of 12 downstream image classification tasks [7, 32, 5, 57, 31, 36, 14, 41, 20, 39]. Table 3 shows the results of four models based on a ViT/B-16 backbone. We perform linear evaluation (See appendix for details on the metrics used to evaluate each of these models). We train two models using two video datasets. The first model is a baseline MAE model pre-trained on randomly sampled frames from the videos on the Moments in time dataset and the Kinetics-400 dataset. The second model is our full ViC-MAE model pre-trained on each of the same two datasets. Our model significantly outperforms the other baselines on 9 out of 12 datasets, whereas the MAE trained on Kinetics is superior on only 3 (i.e. Cars, Aircraft and Pets).

5.3. Ablations

We investigate in this section the effect of various frame-level image transformations used to augment the data, the effect of our choice of frame separation, and the choice of pooling operator.

Augmentations. We perform an ablation study to check whether the use of strong color augmentations on the target encoder is necessary as it is crucial in standard self-supervised methods for images. The results are presented in Table 6. Using only color augmentations meaning that the sampled frame in the target encoder is color augmented

Frame separation	ImageNet-1K	
	Top-1	Top-5
0	63.25	83.34
2	64.47	84.31
4	65.25	84.64
8	65.89	84.91
D	67.66	86.22

Table 4: **Ablation on frame separation.** Linear evaluation on the ImageNet-1K dataset using different frame separation. 0 means sample the same frame. D stands for distant sampling and the rest are using continuous sampling.

but not spatially augmented the performance is reduced by $> 2\%$ on linear evaluation on the Imagenet dataset. Using a combination of strong color augmentations and spatial augmentations, though it increases performance; it is not superior to using only strong spatial augmentations. This is stark contrast with previous methods that necessitate strong color augmentation to be able to learn using contrastive learning. In the following experiments, we only use strong spatial augmentations and discard the use of color augmentations entirely.

Frame separation. This is an essential design component of our framework, and in this experiment we aim to see the effect of frame separation on the performance of our method. We follow the two methods of sampling frames from Xu et.al [58]. Results are shown in Table 4. The first method is *Continuous sampling*, which consists in selecting a starting index i and then sampling a frame in the interval $(i, i + \delta]$, where δ is the frame separation. A frame separation of 0 indicates that the predictor and the target networks receive the same frame. The second method is *distant sampling*, where the video is split into n intervals of the same size, where n is the number of frames to use for contrastive learning and then one frame is selected randomly from each interval. In our experiment, we observe that increasing the frame separation when using *continuous sampling* increases the performance of the model. We observe the best perfor-

Model	Pooling type	ImageNet-1K	
		Top-1	Top-5
ViC-MAE (Ours)	GeM	66.92	85.50
ViC-MAE (Ours)	max	67.01	85.59
ViC-MAE (Ours)	mean	67.66	86.22

Table 5: **Ablation on pooling type.** Linear evaluation on the ImageNet-1K dataset using different types of pooling. The hyperparameter λ is set to 0.025 and introduced using an schedule.

mance using *distant sampling* with $n = 2$ (labelled D in Table 4). We posit that further increasing frame separation offers potentially stronger augmentations. In the following experiments, we only use strong spatial augmentations combined with distant frame sampling.

Pooling type. Since this is an important step in our proposed method, we test which operator Ω used to aggregate local features performs best at producing global features. We report our results in Table 5. We try common types of pooling (*mean*, *max*) as well as, *generalized mean pooling*. We found *mean* to be more effective in creating a global representation for the video, and we use it for all other experiments.

5.4. Limitations

Having shown that ViC-MAE is able to learn useful representations from video data that transfer well to image classification and that surpasses previous models on the same set-up, we contextualize our results by discussing state of the art results in these problems and limitations of our method.

Comparing with models of a similar computational budget our model is able to perform on par with previous results on the Kinetics-400 dataset. However, compared to TubeViT [44] our model still underperforms by 7.1% points in absolute accuracy. A model that works well across both images and video might still need pre-training in both domains. Compared to MaskFeat [55], our model underperforms by 0.7% points in absolute accuracy (82.2% vs. 81.5%). Our model nevertheless is able to surpass the MViTv1-B model [19], the TimeSformer model [6] and the ViVit-B model [2] by 0.3%, 0.8%, and 1.5% points in absolute accuracy respectively (81.2%, 80.7%, and 80% vs. 81.5%). Compared to models that only perform contrastive learning on videos our model underperforms compared to DINO [8] by 1% points in absolute accuracy (82.5% vs. 81.5%). These results contextualize ViC-MAE against high performing models that are using either stronger backbones or additional supervision. We posit that a model trained on a combination of video and image data is likely to perform best across domains.

Finally, we compare our ViC-MAE to a number of state of the art in-domain Imagenet-pretrained models trained with a

Color Augm.	Spatial Augm.	ImageNet-1K	
		Top-1	Top-5
✓		65.40	84.03
	✓	67.66	86.22
✓	✓	66.03	85.01

Table 6: **Ablation on different augmentations.** Linear evaluation on the ImageNet-1K dataset using different augmentations. Color augs include random color jitter, grayscale conversion and gaussian blur. Spatial augs are random re-sized crop and horizontal flip.

similar computational budget. We found that most models trained on video including our model, underperform most of the models in this category. The domain gap between any video dataset and images on Imagenet-1k still seems not to have been closed. Compared to a model that uses masked image modeling, the original MAE [27] and to the MaskFeat model [55], our model underperforms by 0.7% points in absolute accuracy (83.6% & 83.6% vs. 82.98%, respectively). Compared to a model that uses contrastive learning, DINO [8], MoCov2 [11], and BeiT [3] our model underperforms by 1.1%, 1%, and 0.3% points in absolute accuracy (84 %, 83.9%, and 83.2% vs 82.9% respectively). These results show that the gap from models pre-trained purely on video still exists but we believe ViC-MAE is a step forward in closing that gap.

6. Conclusion

In this work, we have introduced ViC-MAE, a method that allows to use unlabeled videos to learn useful representation for image recognition tasks. We achieve this randomly sampling frames from a video and using contrastive learning to pull together frames from the same video and push apart frames from different videos, likewise we also use masked image modeling on each frame to learn good local features of the scene presented in each frame. The main contribution of our work is showing that is possible to combine masked image modeling and contrastive learning by pooling the local representations of the MAE prediction heads into a global representation that is used for contrastive learning. The design choices that we have taken, when designing ViC-MAE show that our work is easily extensible in various different ways. For example, improvements in contrastive learning for images can be directly adapted into our framework. Likewise, pixel reconstruction can be replaced by features that are important for video representation like object correspondence, or optical flow.

Acknowledgements

The authors would like to thank Google Cloud and the CURE program from Google Research for providing funding for this research effort. We are also thankful for support from the Department of Computer Science at Rice University.

References

- [1] Pulkit Agrawal, Joao Carreira, and Jitendra Malik. Learning to see by moving. In *Proceedings of the IEEE international conference on computer vision*, pages 37–45, 2015. [2](#)
- [2] Anurag Arnab, Mostafa Dehghani, Georg Heigold, Chen Sun, Mario Lučić, and Cordelia Schmid. Vivit: A video vision transformer. In *Proceedings of the IEEE/CVF international conference on computer vision*, pages 6836–6846, 2021. [8](#)
- [3] Hangbo Bao, Li Dong, and Furu Wei. Beit: Bert pre-training of image transformers. *arXiv preprint arXiv:2106.08254*, 2021. [1](#), [8](#), [12](#)
- [4] Adrien Bardes, Jean Ponce, and Yann LeCun. Vi-creg: Variance-invariance-covariance regularization for self-supervised learning. *arXiv preprint arXiv:2105.04906*, 2021. [1](#), [2](#), [4](#), [5](#), [6](#), [7](#), [12](#)
- [5] Thomas Berg, Jiongxin Liu, Seung Woo Lee, Michelle L Alexander, David W Jacobs, and Peter N Belhumeur. Birdsnap: Large-scale fine-grained visual categorization of birds. In *Proceedings of the IEEE Conference on Computer Vision and Pattern Recognition*, pages 2011–2018, 2014. [7](#)
- [6] Gedas Bertasius, Heng Wang, and Lorenzo Torresani. Is space-time attention all you need for video understanding? In *ICML*, volume 2, page 4, 2021. [8](#)
- [7] Lukas Bossard, Matthieu Guillaumin, and Luc Van Gool. Food-101—mining discriminative components with random forests. In *Computer Vision—ECCV 2014: 13th European Conference, Zurich, Switzerland, September 6–12, 2014, Proceedings, Part VI 13*, pages 446–461. Springer, 2014. [7](#)
- [8] Mathilde Caron, Hugo Touvron, Ishan Misra, Hervé Jégou, Julien Mairal, Piotr Bojanowski, and Armand Joulin. Emerging properties in self-supervised vision transformers. In *Proceedings of the IEEE/CVF International Conference on Computer Vision*, pages 9650–9660, 2021. [1](#), [8](#)
- [9] Mark Chen, Alec Radford, Rewon Child, Jeffrey Wu, Heewoo Jun, David Luan, and Ilya Sutskever. Generative pretraining from pixels. In *International conference on machine learning*, pages 1691–1703. PMLR, 2020. [12](#)
- [10] Ting Chen, Simon Kornblith, Mohammad Norouzi, and Geoffrey Hinton. A simple framework for contrastive learning of visual representations. In *International conference on machine learning*, pages 1597–1607. PMLR, 2020. [1](#), [4](#), [5](#)
- [11] Xinlei Chen, Haoqi Fan, Ross Girshick, and Kaiming He. Improved baselines with momentum contrastive learning. *arXiv preprint arXiv:2003.04297*, 2020. [8](#)
- [12] Xinlei Chen and Kaiming He. Exploring simple siamese representation learning. In *Proceedings of the IEEE/CVF Conference on Computer Vision and Pattern Recognition*, pages 15750–15758, 2021. [1](#), [2](#), [4](#), [5](#), [6](#), [7](#), [12](#)
- [13] Xinlei Chen, Saining Xie, and Kaiming He. An empirical study of training self-supervised vision transformers. In *Proceedings of the IEEE/CVF International Conference on Computer Vision*, pages 9640–9649, 2021. [12](#)
- [14] Mircea Cimpoi, Subhansu Maji, Iasonas Kokkinos, Sammy Mohamed, and Andrea Vedaldi. Describing textures in the wild. In *Proceedings of the IEEE conference on computer vision and pattern recognition*, pages 3606–3613, 2014. [7](#)
- [15] Kevin Clark, Minh-Thang Luong, Quoc V Le, and Christopher D Manning. Electra: Pre-training text encoders as discriminators rather than generators. *arXiv preprint arXiv:2003.10555*, 2020. [12](#)
- [16] Ekin D Cubuk, Barret Zoph, Jonathon Shlens, and Quoc V Le. Randaugment: Practical automated data augmentation with a reduced search space. In *Proceedings of the IEEE/CVF conference on computer vision and pattern recognition workshops*, pages 702–703, 2020. [12](#)
- [17] Ali Diba, Vivek Sharma, Luc Van Gool, and Rainer Stiefelhagen. Dynamonet: Dynamic action and motion network. In *ICCV*, 2019. [2](#)
- [18] Alexey Dosovitskiy, Lucas Beyer, Alexander Kolesnikov, Dirk Weissenborn, Xiaohua Zhai, Thomas Unterthiner, Mostafa Dehghani, Matthias Minderer, Georg Heigold, Sylvain Gelly, et al. An image is worth 16x16 words: Transformers for image recognition at scale. *arXiv preprint arXiv:2010.11929*, 2020. [2](#), [5](#), [12](#)
- [19] Haoqi Fan, Bo Xiong, Karttikeya Mangalam, Yanghao Li, Zhicheng Yan, Jitendra Malik, and Christoph Feichtenhofer. Multiscale vision transformers. In *Proceedings of the IEEE/CVF International Conference on Computer Vision*, pages 6824–6835, 2021. [8](#)
- [20] Li Fei-Fei, Rob Fergus, and Pietro Perona. Learning generative visual models from few training examples: An incremental bayesian approach tested on 101 object categories. In *2004 conference on computer vision and pattern recognition workshop*, pages 178–178. IEEE, 2004. [7](#)
- [21] Christoph Feichtenhofer, Haoqi Fan, Yanghao Li, and Kaiming He. Masked autoencoders as spatiotemporal learners. *arXiv preprint arXiv:2205.09113*, 2022. [1](#), [2](#), [3](#), [6](#), [12](#)
- [22] Christoph Feichtenhofer, Haoqi Fan, Bo Xiong, Ross Girshick, and Kaiming He. A large-scale study on unsupervised spatiotemporal representation learning. In *Proceedings of the IEEE/CVF Conference on Computer Vision and Pattern Recognition*, pages 3299–3309, 2021. [1](#)
- [23] Xavier Glorot and Yoshua Bengio. Understanding the difficulty of training deep feedforward neural networks. In *Proceedings of the thirteenth international conference on artificial intelligence and statistics*, pages 249–256. JMLR Workshop and Conference Proceedings, 2010. [12](#)
- [24] Daniel Gordon, Kiana Ehsani, Dieter Fox, and Ali Farhadi. Watching the world go by: Representation learning from unlabeled videos. *arXiv preprint arXiv:2003.07990*, 2020. [2](#), [3](#), [6](#)
- [25] Priya Goyal, Piotr Dollár, Ross Girshick, Pieter Noordhuis, Lukasz Wesolowski, Aapo Kyrola, Andrew Tulloch, Yangqing Jia, and Kaiming He. Accurate, large mini-batch sgd: Training imagenet in 1 hour. *arXiv preprint arXiv:1706.02677*, 2017. [12](#)

- [26] Jean-Bastien Grill, Florian Strub, Florent Althé, Corentin Tallec, Pierre Richemond, Elena Buchatskaya, Carl Doersch, Bernardo Avila Pires, Zhaohan Guo, Mohammad Gheshlaghi Azar, et al. Bootstrap your own latent—a new approach to self-supervised learning. *Advances in neural information processing systems*, 33:21271–21284, 2020. 4
- [27] Kaiming He, Xinlei Chen, Saining Xie, Yanghao Li, Piotr Dollár, and Ross Girshick. Masked autoencoders are scalable vision learners. In *Proceedings of the IEEE/CVF Conference on Computer Vision and Pattern Recognition*, pages 16000–16009, 2022. 1, 2, 6, 7, 8, 12
- [28] Kaiming He, Haoqi Fan, Yuxin Wu, Saining Xie, and Ross Girshick. Momentum contrast for unsupervised visual representation learning. In *Proceedings of the IEEE/CVF conference on computer vision and pattern recognition*, pages 9729–9738, 2020. 1
- [29] Gao Huang, Yu Sun, Zhuang Liu, Daniel Sedra, and Kilian Q Weinberger. Deep networks with stochastic depth. In *Computer Vision—ECCV 2016: 14th European Conference, Amsterdam, The Netherlands, October 11–14, 2016, Proceedings, Part IV 14*, pages 646–661. Springer, 2016. 12
- [30] Will Kay, Joao Carreira, Karen Simonyan, Brian Zhang, Chloe Hillier, Sudheendra Vijayanarasimhan, Fabio Viola, Tim Green, Trevor Back, Paul Natsev, Mustafa Suleyman, and Andrew Zisserman. The kinetics human action video dataset, 2017. 6
- [31] Jonathan Krause, Michael Stark, Jia Deng, and Li Fei-Fei. 3d object representations for fine-grained categorization. In *Proceedings of the IEEE international conference on computer vision workshops*, pages 554–561, 2013. 7
- [32] Alex Krizhevsky, Geoffrey Hinton, et al. Learning multiple layers of features from tiny images. 2009. 7
- [33] Ilya Loshchilov and Frank Hutter. Sgdr: Stochastic gradient descent with warm restarts. *arXiv preprint arXiv:1608.03983*, 2016. 12
- [34] Ilya Loshchilov and Frank Hutter. Decoupled weight decay regularization. *arXiv preprint arXiv:1711.05101*, 2017. 12
- [35] William Lotter, Gabriel Kreiman, and David Cox. Deep predictive coding networks for video prediction and unsupervised learning. In *ICLR*, 2017. 2
- [36] Subhransu Maji, Esa Rahtu, Juho Kannala, Matthew Blaschko, and Andrea Vedaldi. Fine-grained visual classification of aircraft. *arXiv preprint arXiv:1306.5151*, 2013. 7
- [37] Michael Mathieu, Camille Couprie, and Yann LeCun. Deep multi-scale video prediction beyond mean square error. In *ICLR*, 2016. 2
- [38] Mathew Monfort, Alex Andonian, Bolei Zhou, Kandan Ramakrishnan, Sarah Adel Bargal, Tom Yan, Lisa Brown, Quanfu Fan, Dan Gutfreund, Carl Vondrick, and Aude Oliva. Moments in time dataset: One million videos for event understanding. *IEEE Transactions on Pattern Analysis and Machine Intelligence*, 42(2):502–508, 2020. 6
- [39] Maria-Elena Nilsback and Andrew Zisserman. Automated flower classification over a large number of classes. In *2008 Sixth Indian Conference on Computer Vision, Graphics & Image Processing*, pages 722–729. IEEE, 2008. 7
- [40] Aaron van den Oord, Yazhe Li, and Oriol Vinyals. Representation learning with contrastive predictive coding. *arXiv preprint arXiv:1807.03748*, 2018. 4
- [41] Omkar M Parkhi, Andrea Vedaldi, Andrew Zisserman, and CV Jawahar. Cats and dogs. In *2012 IEEE conference on computer vision and pattern recognition*, pages 3498–3505. IEEE, 2012. 7
- [42] Nikhil Parthasarathy, SM Eslami, João Carreira, and Olivier J Hénaff. Self-supervised video pretraining yields strong image representations. *arXiv preprint arXiv:2210.06433*, 2022. 2, 3
- [43] Deepak Pathak, Ross Girshick, Piotr Dollár, Trevor Darrell, and Bharath Hariharan. Learning features by watching objects move. In *Proceedings of the IEEE conference on computer vision and pattern recognition*, pages 2701–2710, 2017. 2
- [44] AJ Piergiovanni, Weicheng Kuo, and Anelia Angelova. Rethinking video vits: Sparse video tubes for joint image and video learning. *arXiv preprint arXiv:2212.03229*, 2022. 3, 6, 8
- [45] Rui Qian, Tianjian Meng, Boqing Gong, Ming-Hsuan Yang, Huisheng Wang, Serge Belongie, and Yin Cui. Spatiotemporal contrastive video representation learning. In *Proceedings of the IEEE/CVF Conference on Computer Vision and Pattern Recognition*, pages 6964–6974, 2021. 1
- [46] Filip Radenović, Giorgos Tolias, and Ondřej Chum. Fine-tuning cnn image retrieval with no human annotation. *IEEE transactions on pattern analysis and machine intelligence*, 41(7):1655–1668, 2018. 5
- [47] Nitish Srivastava, Elman Mansimov, and Ruslan Salakhudinov. Unsupervised learning of video representations using lstms. In *International conference on machine learning*, pages 843–852. PMLR, 2015. 2
- [48] Christian Szegedy, Vincent Vanhoucke, Sergey Ioffe, Jon Shlens, and Zbigniew Wojna. Rethinking the inception architecture for computer vision. In *Proceedings of the IEEE conference on computer vision and pattern recognition*, pages 2818–2826, 2016. 12
- [49] Yonglong Tian, Olivier J Henaff, and Aaron van den Oord. Divide and contrast: Self-supervised learning from uncurated data. In *Proceedings of the IEEE/CVF International Conference on Computer Vision*, pages 10063–10074, 2021. 2
- [50] Zhan Tong, Yibing Song, Jue Wang, and Limin Wang. Videomae: Masked autoencoders are data-efficient learners for self-supervised video pre-training. In *NeurIPS*, 2022. 2
- [51] Carl Vondrick, Hamed Pirsiavash, and Antonio Torralba. Anticipating visual representations from unlabelled video. In *CVPR*, 2016. 2
- [52] Jacob Walker, Carl Doersch, Abhinav Gupta, and Martial Hebert. An uncertain future: Forecasting from static images using variational autoencoders. In *ICCV*, 2016. 2
- [53] Xiaolong Wang and Abhinav Gupta. Unsupervised learning of visual representations using videos. In *ICCV*, 2015. 2
- [54] Xiaolong Wang, Allan Jabri, , and Alexei A. Efros. Learning correspondence from the cycle consistency of time. In *CVPR*, 2019. 2
- [55] Chen Wei, Haoqi Fan, Saining Xie, Chao-Yuan Wu, Alan Yuille, and Christoph Feichtenhofer. Masked feature prediction for self-supervised visual pre-training. In *Proceedings of*

the IEEE/CVF Conference on Computer Vision and Pattern Recognition, pages 14668–14678, 2022. [1](#), [2](#), [8](#)

- [56] Haiping Wu and Xiaolong Wang. Contrastive learning of image representations with cross-video cycle-consistency. In *Proceedings of the IEEE/CVF International Conference on Computer Vision*, pages 10149–10159, 2021. [2](#), [3](#), [6](#)
- [57] Jianxiong Xiao, James Hays, Krista A Ehinger, Aude Oliva, and Antonio Torralba. Sun database: Large-scale scene recognition from abbey to zoo. In *2010 IEEE computer society conference on computer vision and pattern recognition*, pages 3485–3492. IEEE, 2010. [7](#)
- [58] Jiarui Xu and Xiaolong Wang. Rethinking self-supervised correspondence learning: A video frame-level similarity perspective. In *Proceedings of the IEEE/CVF International Conference on Computer Vision*, pages 10075–10085, 2021. [2](#), [3](#), [4](#), [6](#), [7](#)
- [59] Hongyi Zhang, Moustapha Cisse, Yann N Dauphin, and David Lopez-Paz. mixup: Beyond empirical risk minimization. *arXiv preprint arXiv:1710.09412*, 2017. [12](#)

A. Implementation Details

We will release code and weights, along with the specific configurations. We follow very similar configurations to [27, 21], since we found them to also work well for ViC-MAE.

ViC-MAE architecture. We follow the standard ViT architecture [18], which has a stack of Transformer blocks, each of which consists of a multi-head attention block and an MLP block, with LayerNorm (LN). A linear projection layer is used after the encoder to match the width of the decoder. We use sine-cosine position embeddings for both the encoder and decoder. For the projection and target networks, we do average pooling on the encoder features and follow the architecture of [4], which consist of linear layer projecting the features up to twice the size of the encoder and two blocks of linear layer the preserve the size of the features, followed by BatchNormalization and a ReLU non-linearity.

We extract features from the encoder output for fine-tuning and linear probing. We use the class token from the original ViT architecture, but remark that similar results are obtained without it (using average pooling).

Pre-training. The default settings can be found in Table 7. We do not perform any color augmentation, drop path or gradient clipping. We initialize our transformer layer using xavier_uniform [23], as it is standard for Transformer architectures. We use the linear lr scaling rule [25]: $lr = base_lr \times batchsize / 256$.

End-to-end finetuning. We follow common practice for end-to-end finetuning. Default settings can be found in Table 8. Similar to [27], we use layer-wise lr decay.

Linear evaluation. We follow [27, 21] for linear evaluation results. As previous work has found [13], we do not use common regularization techniques, mixup, cutmix, and drop path, likewise, we set the weight decay to zero. We add an extra BatchNorm layer without the affine transformation after the encoder features. Default settings can be found in Table 9.

B. Semi-supervised evaluation on ImageNet.

We also test ViC-MAE on the problem of Semi-Supervised evaluation on the ImageNet dataset. The setting consists on training on a subset of the training data and testing on the whole validation data. We chose subsets of size 5%, 10%, 25%, 50%, 75% and 100% of the whole training set of ImageNet. We compare our model against MAE [27] + SiamSiam [12], and MAE [27] + VicReg [4]. Results are shown on Table 10, and show the superiority of ViC-MAE over simple combinations of contrastive learning and masked image modeling.

config	value
optimizer	AdamW [34]
base learning rate	1.5e-4
weight decay	0.05
optimizer momentum	$\beta_1, \beta_2=0.9, 0.95$ [9]
batch size	4096
learning rate schedule	cosine decay [33]
warmup epochs [25]	40
epochs	800
augmentation	hflip, crop [0.5, 1]
contrastive loss weight λ	0.025
contrastive loss schedule	0 until epoch 200 then 0.025

Table 7: **Pre-training setting.**

config	value
optimizer	AdamW
base learning rate	1e-3
weight decay	0.05
optimizer momentum	$\beta_1, \beta_2=0.9, 0.999$
layer-wise lr decay [15, 3]	0.75
batch size	1024
learning rate schedule	cosine decay
warmup epochs	5
training epochs	100
augmentation	RandAug (9, 0.5) [16]
label smoothing [48]	0.1
mixup [59]	0.8
drop path [29]	0.1

Table 8: **End-to-end fine-tuning setting.**

config	value
optimizer	SGD
base learning rate	0.1
weight decay	0
optimizer momentum	0.9
batch size	4096
learning rate schedule	cosine decay
warmup epochs	10
training epochs	90
augmentation	RandomResizedCrop

Table 9: **Linear evaluation setting.**

Percentage of data	5%	10%	25%	50%	75%	100%
MAE [27] + SiamSiam [12]	7.15	23.41	39.73	54.94	62.88	67.44
MAE [27] + VicReg [4]	47.48	56.63	66.62	73.00	75.29	77.41
ViC-MAE (ours)	50.25	58.22	67.65	73.97	75.80	77.89

Table 10: **Semi-supervised evaluation on ImageNet.** We performed end-to-end finetuning using the settings in 8, but disable RandAug and MixUp for this experiment.